

Preparation and Structure of $[\text{Rh}_3(\mu\text{-}(\text{Ph}_2\text{PCH}_2)_2\text{PPh})_2(\mu\text{-CO})(\text{CO})(\mu\text{-X})\text{X}][\text{BPh}_4]$ (X = Cl, Br, I), a Ligand-Poor Set of Trirhodium Clusters

Alan L. Balch,* L. Alan Fossett, Rosalvina R. Guimerans, and Marilyn M. Olmstead

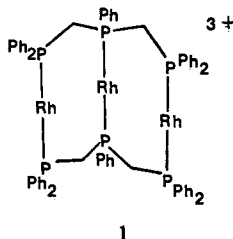
Department of Chemistry, University of California, Davis, California 95616

Received August 6, 1984

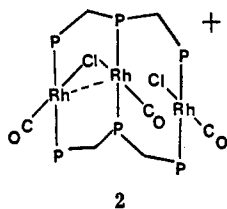
Mild heating (60–80 °C) of $[\text{Rh}_3(\mu\text{-dpmp})_2(\text{CO})_3\text{X}_2][\text{BPh}_4]$ (dpmp is bis[(diphenylphosphino)methyl]phenylphosphine; X = Cl, Br, I) in solution for 12–48 h results in carbon monoxide loss and the formation of $[\text{Rh}_3(\mu\text{-dpmp})_2(\mu\text{-CO})(\text{CO})(\mu\text{-X})\text{X}][\text{BPh}_4]$. The infrared, electronic, and NMR (^1H , ^{13}C , ^{31}P) spectra of these complexes indicate that they have a common, rigid structure. The structure of $[\text{Rh}_3(\mu\text{-dpmp})_2(\mu\text{-CO})(\text{CO})(\mu\text{-Cl})(\text{Cl})][\text{BPh}_4]\cdot\text{CH}_2\text{Cl}_2$ has been determined by X-ray crystallography. The compound crystallizes from dichloromethane–ether in the monoclinic space group $P2_1/n$, a nonstandard setting of $P2_1/c$ (No. 14), with four molecules per unit cell of dimensions $a = 22.015$ (8), $b = 15.002$ (4) Å, $c = 26.084$ (8) Å, and $\beta = 106.95$ (2)° at 140 K. Least-squares refinement of 495 parameters using 7796 reflections yields $R = 0.072$. The structure consists of a bent Rh_3 chain with trans triphosphines and a bonding $\text{Rh}\text{-Rh}$ separation of 2.704 Å for the segment bridged by carbon monoxide and a nonbonded $\text{Rh}\cdots\text{Rh}$ separation of 2.966 Å for the part bridged by a chloride ligand. The structure is comprised of units which are geometrically similar to previously characterized binuclear and mononuclear complexes.

Introduction

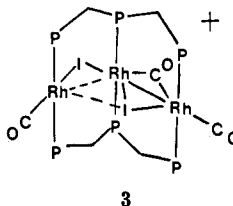
We have recently described the preparation of trirhodium complexes of the linear, small bite ligand, bis[(diphenylphosphino)methyl]phenylphosphine (dpmp).^{1–5} These aggregates contain a structurally stable $\text{Rh}_3(\mu\text{-dpmp})_2^{3+}$ core, 1, with additional ligands binding in the



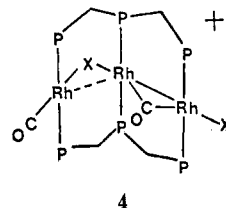
plane perpendicular to the P–Rh–P units. For the tricarbonyl complexes $[\text{Rh}_3(\mu\text{-dpmp})_2(\text{CO})_3\text{X}_2]^+$, the structure is sensitive to the nature of the monoanionic ligand X. With chloride as X the cation has the structure 2.¹ In



solution the bridging and terminal chloride ligands of 2 undergo rapid exchange. However with iodide as X the corresponding cation has the rigid structure 3 with a much



different array of bridging ligands and a more substantially bent $\text{Rh}\text{-Rh}\text{-Rh}$ unit.² The bromo complex adopts yet another structure that allows for rapid bridge/terminal carbonyl exchange.^{2,6} We have briefly reported⁴ that 3 can lose carbon monoxide (reversibly) to form the dicarbonyl cation $[\text{Rh}_3(\mu\text{-dpmp})_2(\mu\text{-CO})(\text{CO})(\mu\text{-I})\text{I}]^+$. Here we report details on the preparation and structure of the three dicarbonyl cations $[\text{Rh}_3(\mu\text{-dpmp})_2(\mu\text{-CO})(\text{CO})(\mu\text{-X})\text{X}]^+$ (X = Cl, Br, I). In contrast to the situation with the tricarbonyl cluster family, these dicarbonyls all have the same basic structure 4 for each of the three halide ligands.



Results

Preparation and Spectroscopic Characterization of $[\text{Rh}_3(\mu\text{-dpmp})_2(\mu\text{-CO})(\text{CO})(\mu\text{-X})\text{X}][\text{BPh}_4]$ (X = Cl, Br, I). Each of the tricarbonyl cations $\text{Rh}_3(\mu\text{-dpmp})_2(\text{CO})_3\text{X}_2]^+$ loses carbon monoxide upon mild heating (60–80 °C) in solution for a 12–48-h period, and the dicarbonyl products are readily isolated in good yield. Upon the addition of carbon monoxide $[\text{Rh}_3(\mu\text{-dpmp})_2(\mu\text{-CO})(\text{CO})(\mu\text{-X})\text{X}]^+$ is converted to $[\text{Rh}_3(\mu\text{-dpmp})_2(\text{CO})_3\text{X}_2]^+$, which may then be reisolated.

Spectroscopic data indicate that the three dicarbonyl species have similar structures. As can be seen in Figure 1, the electronic spectra of the cations are all very similar. In contrast the electronic spectra of the three tricarbonyl cations are each distinctive and different from those of the dicarbonyls.⁷ The infrared spectra of the dicarbonyls given in Table I show the presence of one band in the terminal carbonyl region and one in the bridging carbonyl region. The ^{31}P NMR spectra indicate that there are three unique phosphorus environments. The ^{31}P NMR spectrum

(1) Guimerans, R. R.; Olmstead, M. M.; Balch, A. L. *J. Am. Chem. Soc.* **1983**, *105*, 1677.

(2) Olmstead, M. M.; Guimerans, R. R.; Balch, A. L. *Inorg. Chem.* **1983**, *22*, 2473.

(3) Balch, A. L.; Olmstead, M. M.; Guimerans, R. R. *Inorg. Chim. Acta* **1984**, *84*, L21.

(4) Balch, A. L.; Guimerans, R. R.; Olmstead, M. M. *J. Organomet. Chem.* **1984**, *268*, C38.

(5) Balch, A. L.; Olmstead, M. M. *Isr. J. Chem.*, in press.

(6) Balch, A. L.; Guimerans, R. R.; Wood, F. E., unpublished results.

(7) Nguyen, M. V. M.S. Thesis, University of California, Davis, CA, 1983.

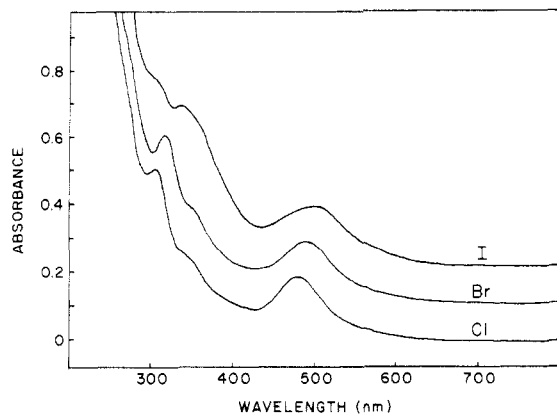


Figure 1. The electronic spectra of 2.2×10^{-4} M dichloromethane solutions of Cl, $[\text{Rh}_3(\mu\text{-dpmp})_2(\mu\text{-CO})(\text{CO})(\mu\text{-Cl})\text{Cl}]^+$, Br, $[\text{Rh}_3(\mu\text{-dpmp})_2(\mu\text{-CO})(\text{CO})(\mu\text{-Br})\text{Br}]^+$, and I, $[\text{Rh}_3(\mu\text{-dpmp})_2(\mu\text{-CO})(\text{CO})(\mu\text{-Cl})\text{Cl}]^+$, at 25 °C with 1.0-mm path length cells.

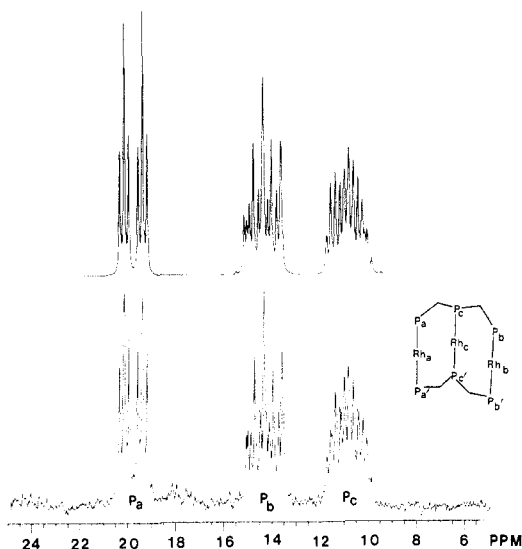


Figure 2. The 145.8-MHz ^{31}P NMR spectrum of a dichloromethane solution of $[\text{Rh}_3(\mu\text{-dpmp})_2(\mu\text{-CO})(\text{CO})(\mu\text{-I})\text{I}][\text{BPh}_4]$. The simulated spectrum at the top was computed by using the parameters: $\delta(\text{P}_a)$ 19.86 ppm; $\delta(\text{P}_b)$ 14.4; $\delta(\text{P}_c)$ 10.9; $J(\text{Rh}_a\text{P}_a)$ = 111.5 Hz; $J(\text{Rh}_b\text{P}_b)$ = 109.9; $J(\text{Rh}_c\text{P}_c)$ = 109.4; $J(\text{P}_a\text{P}_c)$ = 28.1; $J(\text{P}_a\text{P}_b)$ = 82.0; $J(\text{P}_a\text{P}_c')$ = 26.9; $J(\text{P}_c\text{P}_b')$ = 28.5; $J(\text{P}_a\text{P}_b)$ = 0.6; $J(\text{P}_a\text{P}_a')$ = 349; $J(\text{P}_c\text{P}_c')$ = 347; $J(\text{P}_b\text{P}_b)$ = 348.

of $[\text{Rh}_3(\mu\text{-dpmp})_2(\mu\text{-CO})(\text{CO})(\mu\text{-I})\text{I}][\text{BPh}_4]$ is shown in Figure 2. The resonance centered at 19.9 ppm, P_a , is clearly assignable to a pair of terminal phosphorus atoms with coupling to the directly bound rhodium ($^1J(\text{Rh}_a\text{P}_a)$ = 110.8 Hz) and coupling to the two, virtually equivalent, interior phosphorus atoms. The resonance centered at 14.4 ppm can be assigned to the other terminal phosphorus atoms. The complex resonance at 10.9 ppm, P_c , is due to the pair of equivalent internal phosphorus atoms. The ^{31}P NMR spectrum has been simulated by using parameters given in the caption to Figure 2. The simulated spectrum is shown at the top of the figure. The coupling constants obtained from this simulation are all consistent with values obtained previously for similar molecules.⁸⁻¹⁰ The symmetry within the ^{31}P NMR spectrum is in accord with the structure found within the solid state. It is not however possible at this stage to make an unambiguous assignment of P_a and P_a' to either set of terminal phosphorus atoms

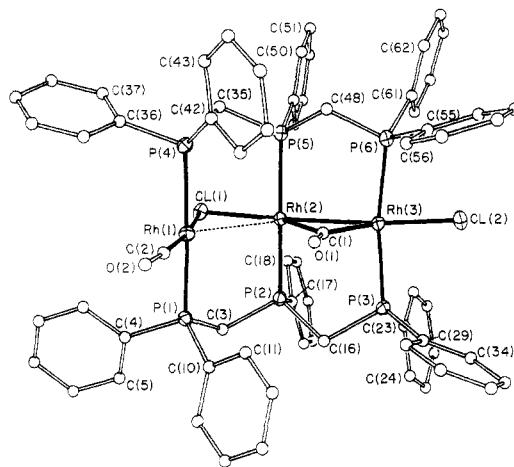


Figure 3. A perspective view of $[\text{Rh}_3(\mu\text{-dpmp})_2(\mu\text{-CO})(\text{CO})(\mu\text{-Cl})\text{Cl}]^+$.

($\text{P}(1),\text{P}(4)$ or $\text{P}(3),\text{P}(6)$) because distinguishing characteristics are not present in the spectra. In particular the consistency in the values of $^1J(\text{Rh},\text{P})$ should be noted. The ^1H NMR spectra of dicarbonyls show the presence of four multiplets (with H,H and P,H coupling) due to the methylene protons along with a complex series of resonances in the phenyl region. The methylene groups are diastereotopic in the free ligand so that two methylene resonances are always expected. The presence of four methylene resonances in this case indicates that the two ends of the ligand are in unique environments. Decoupling experiments have allowed us to assign some resonances (see Table I) to coupled methylene groups. The ^{13}C NMR spectrum of ^{13}C -enriched $[\text{Rh}_3(\mu\text{-dpmp})_2(\mu\text{-CO})(\text{CO})(\mu\text{-Br})\text{Br}]^+$ in dichloromethane solution at 23 °C shows the presence of resonances due to terminal and bridging carbon monoxide in 1:1 ratio. The resonance of the terminal carbonyl appears as a doublet of triplets at 185.3 ppm with $^1J(\text{C},\text{Rh})$ = 83.6 and $^2J(\text{C},\text{P})$ = 16.1 Hz, while the resonance of the bridging carbonyl appears as a triplet of quintets at 220.1 ppm with $^1J(\text{C},\text{Rh})$ = 46.7 and $^2J(\text{C},\text{P})$ = 6.3 Hz. The nonequivalence of the two rhodium atoms about the bridging carbonyl is not resolved in this spectrum. The magnitudes of $^1J(\text{C},\text{Rh})$ and $^2J(\text{C},\text{P})$ are consistent with earlier findings on related binuclear complexes.⁸⁻¹⁰ All of the NMR (^{31}P , ^1H , and ^{13}C) are unaffected on lowering the temperature to -80 °C. Since these spectra are also wholly in accord with the solid-state structure obtained from X-ray diffraction, we conclude that these dicarbonyls retain a rigid structure in solution.

The X-ray Crystal Structure of $[\text{Rh}_3(\mu\text{-dpmp})_2(\mu\text{-CO})(\text{CO})(\mu\text{-Cl})\text{Cl}][\text{BPh}_4]\cdot\text{CH}_2\text{Cl}_2$. The structure consists of the cation, the tetraphenyl borate anion and one slightly disordered dichloromethane molecule. There are no unusual contacts between these constituents. A drawing of the cation that gives the atomic numbering scheme is given in Figure 3. Atomic positional parameters are given in Table II. Tables III and IV give selected interatomic distances and angles. Figure 4 shows a stereoscopic view of the cation. There is no imposed crystallographic symmetry. However the cation has a virtual mirror plane passing through the nearly planar $\text{Rh}_3(\text{CO})_2\text{Cl}_2$ unit. This is best appreciated by turning to the stereoscopic view (Figure 4). The near mirror symmetry extends out to include even the phenyl groups. The greatest deviation from this symmetry involves the orientation of the two opposed phenyl groups bound to $\text{P}(1)$ and $\text{P}(4)$. In solution normal molecular motion renders the phosphine ligands fully equivalent.

(8) Mague, J. T.; DeVries, S. H. *Inorg. Chem.* **1982**, *21*, 1632.

(9) Mague, J. T.; DeVries, S. H. *Inorg. Chem.* **1980**, *19*, 3743.

(10) Mague, J. T.; Sanger, A. R. *Inorg. Chem.* **1979**, *18*, 2060.

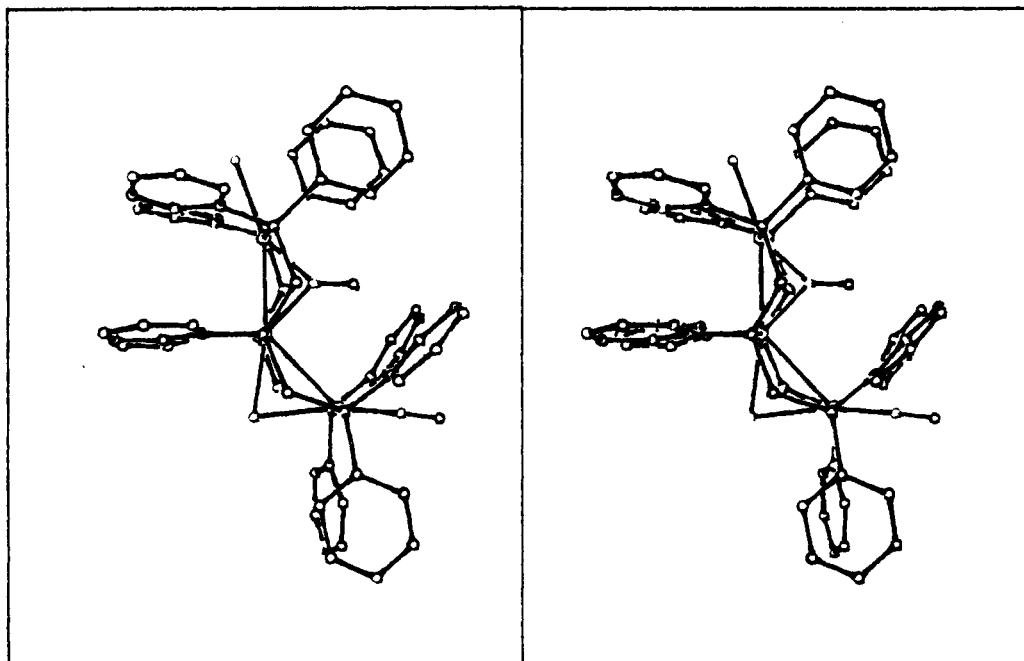


Figure 4. A stereoscopic view of $[\text{Rh}_3(\mu\text{-dpmp})_2(\mu\text{-CO})(\text{CO})(\mu\text{-Cl})\text{Cl}]^+$.

The geometry of the cation is related to the structure of other binuclear rhodium complexes, particularly those bridged by bis(diphenylphosphino)methane (dpm).¹¹ Figure 5 offers a comparison of the structure of 4 ($X = \text{Cl}$) with the structure¹² of the chloro-bridged A-frame $[\text{Rh}_2(\mu\text{-dpm})_2(\mu\text{-Cl})(\text{CO})_2]^+$, on the left, and the carbonyl-bridged A-frame $\text{Rh}_2(\mu\text{-dpm})_2(\mu\text{-CO})\text{Cl}_2$,¹³ on the right. There are striking similarities with both binuclear structures. The left side of 4, including Rh(1) and its ligands as well as Rh(2) and its ligands (except for the bridging carbonyl and Rh(3)), resembles the chloro-bridged A-frame $\text{Rh}_2(\mu\text{-dpm})_2(\mu\text{-Cl})(\text{CO})_2^+$. The right side of 4, including the coordination environments of Rh(3) and Rh(2), maps out structural elements found in $\text{Rh}_2(\mu\text{-dpm})_2(\mu\text{-CO})\text{Cl}_2$. Not only are the coordination environments about rhodium and the in-plane bridging ligand geometry similar but also the dispositions of the bridging phosphines and their phenyl substituents are closely related. In the binuclear A-frames $[\text{Rh}_2(\mu\text{-dpm})_2(\mu\text{-Cl})(\text{CO})_2]^+$ and $\text{Rh}_2(\mu\text{-dpm})_2(\mu\text{-CO})\text{Cl}_2$, the methylene groups of dpm are arranged so that they lie on the same side of the Rh_2P_4 plane as does the bridging chloro or carbonyl group. Consequently the $\text{CP}_2\text{Rh}_2\text{Cl}$ and $\text{CP}_2\text{Rh}_2\text{C}$ rings have boat conformations. This holds true in 4 as well. The methylene bridges are disposed so that they lie directly above the bridging chloro and carbonyl groups. Since these bridging chloro and carbonyl groups lie on opposite sides of an arc connecting Rh(1), Rh(2), and Rh(3), the methylene groups lie on opposite sides of arcs drawn to connect the phosphorus atoms of one ligand.

The geometry of the $\text{Rh}_3(\mu\text{-dpmp})_2$ core is comprised of units of normal structural characteristics. The Rh-P distances fall into a very narrow range, 2.299 (4)–2.324 (4) Å. These distances are comparable to those found in mono-,^{14,15} bi-,^{12,13,16,17} and trinuclear^{1,2} rhodium(I) com-

plexes. The P-Rh-P angles show increasing deviation from linearity as one proceeds from left to right across the molecule as shown in Figure 5. The P(1)-Rh(1)-P(4) angle is 176.7°. For P(2)-Rh(2)-P(5) it is 172.7°, and for P(3)-Rh(3)-P(6) it is 168.3°. Interestingly these angles parallel those in the corresponding binuclear A-frames. In $\text{Rh}_2(\mu\text{-dpm})_2(\mu\text{-Cl})(\text{CO})_2^+$ the P-Rh-P angles are 176.20 and 176.12°¹² while in $\text{Rh}_2(\mu\text{-dpm})_2(\mu\text{-CO})\text{Br}_2$ these angles are 171.41 and 166.78°.¹³ The bending of the P(3)-Rh(3)-P(6) angle is probably a consequence of the short Rh(2)-Rh(3) distance (2.704 (2) Å). This is shorter in 4 than the corresponding nonbonded P(5)···P(6) (2.944 (8) Å) and P(2)···P(3) (2.945 (8) Å) separations. To accommodate the Rh(2)-Rh(3) bond the P(3)-Rh(3)-P(6) angle is bent inward. On the other side of the molecule, the Rh(1)···Rh(2) (2.966 Å), P(1)···P(2) (3.084 (8) Å), and P(4)···P(5) (3.064 (8) Å) separations are more nearly comparable, and no bending of the P-Rh-P angles is necessary. Likewise in $\text{Rh}_2(\mu\text{-dpm})_2(\mu\text{-CO})\text{Br}_2$ the Rh-Rh bond (2.7566 (9) Å) is shorter than the P···P separations (3.026 (3) and 2.992 (3) Å)¹³ whereas in $\text{Rh}_2(\mu\text{-dpm})_2(\mu\text{-Cl})(\text{CO})_2^+$ the nonbonded Rh···Rh separation (3.1520 (8) Å) is slightly longer than the P···P separations (3.088 (2) and 3.097 (2) Å) and no inward bend of the P-Rh-P units is required.¹²

Within each dpmp ligand the structural features are quite regular. All of the phenyl rings are planar. The phosphorus-methylene carbon distances fall in the range 1.821–1.859 Å which is normal. The phosphorus-phenyl carbon distances are normal. The P-C-P angles reflect the rhodium-rhodium separations which they span. In this regard they behave similarly to the methylene groups in dpm.¹⁶ The P(1)-C(3)-P(2) (113.5 (7)°) and P(4)-C(35)-P(5) (111.7 (7)°) angles that span the long Rh(1)···Rh(2) separation are larger than the P(2)-C(16)-P(3) (106.3 (7)°) and the P(5)-C(48)-P(6) (106.1 (6)°) angles that span the shorter Rh(2)-Rh(3) separation. The P(1)-C(3)-P(2) and P(4)-C(35)-P(5) angles are similar to those in $[\text{Rh}_2(\mu\text{-dpm})_2(\mu\text{-Cl})(\text{CO})_2]^+$ (both 114.7 (3)°)¹² while the corresponding angles in $\text{Rh}_2(\mu\text{-dpm})_2(\mu\text{-CO})\text{Br}_2$ (111.0 (4), 109.9 (4)°)¹³ are somewhat larger than the P(2)-C(16)-P(3) and P(5)-C(48)-P(6) angles.

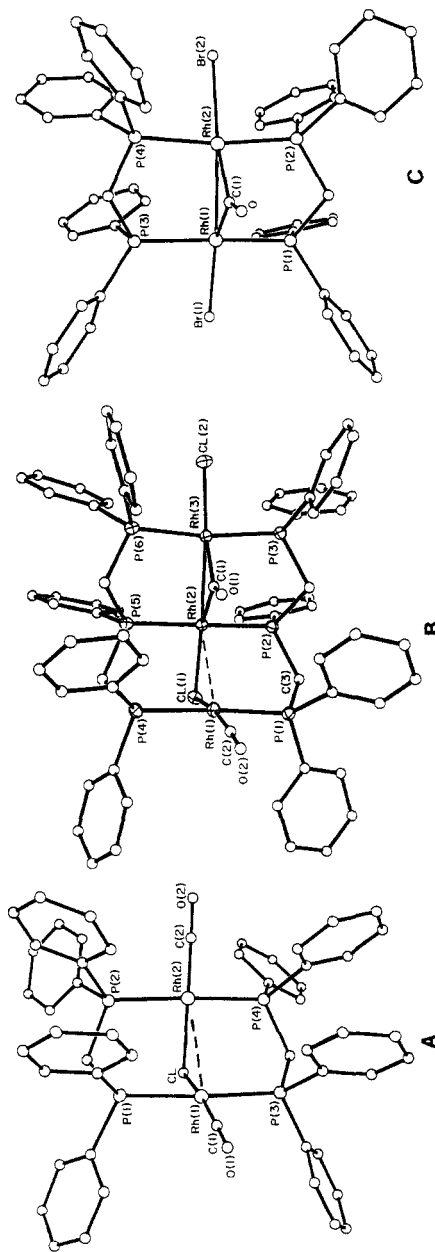
(11) Balch, A. L. In "Homogeneous Catalysis with Metal Phosphine Complexes"; Pignolet, L. H., Ed.; Plenum Press: New York, 1983; p 167.
 (12) Cowie, M.; Dwight, S. K. *Inorg. Chem.* 1979, 18, 2700.
 (13) Cowie, M.; Dwight, S. K. *Inorg. Chem.* 1980, 19, 2508.
 (14) La Placa, S. J.; Ibers, J. A. *Acta Crystallogr.* 1965, 18, 511.
 (15) Bennett, M. J.; Donaldson, P. B. *Inorg. Chem.* 1977, 16, 655.
 (16) Olmstead, M. M.; Lindsay, C. H.; Benner, L. S.; Balch, A. L. *J. Organomet. Chem.* 1979, 179, 289.

(17) Kubiak, C. P.; Eisenberg, R. *Inorg. Chem.* 1980, 19, 2726.

Table I. Spectroscopic Data for $[\text{Rh}_3(\mu\text{-dpmp})_2(\mu\text{-CO})(\text{CO})(\mu\text{-X})] [\text{BPh}_4]$

compound	$\nu(\text{CO}), \text{cm}^{-1}$	^{31}P NMR ^c			^1H NMR ^c			
		$\delta(\text{a})$	$\delta(\text{b})$	$\delta(\text{c})$	$J(\text{Rh}_a\text{P}_a)$	$J(\text{Rh}_b\text{P}_b)$	$J(\text{Rh}_c\text{P}_c)$	J
$[\text{Rh}_3(\mu\text{-dpmp})_2(\mu\text{-CO})(\text{CO})(\mu\text{-Cl})\text{Cl}]^+$	1978, 1780	19.1	18.3	12.9	112.8	117.6	113.2	3.77 ^a
$[\text{Rh}_3(\mu\text{-dpmp})_2(\mu\text{-CO})(\text{CO})(\mu\text{-Br})\text{Br}]^+$	1982, 1780	19.2	17.5	12.5	114.7	112.4	111.5	3.89
$[\text{Rh}_3(\mu\text{-dpmp})_2(\mu\text{-CO})(\text{CO})(\mu\text{-I})\text{I}]^+$	1962, 1782	19.9	14.4	10.9	111.5	109.9	109.4	4.25

^{a, b} Decoupling experiments indicate that these are directly coupled protons of one methylene group. ^c δ in ppm; J in Hz.

Figure 5. A comparison of the structures of A, $[\text{Rh}_2(\mu\text{-dpmp})_2(\mu\text{-Cl})(\text{CO})_2]$, B, $[\text{Rh}_3(\mu\text{-dpmp})_2(\mu\text{-CO})(\text{CO})(\mu\text{-Cl})(\text{Cl})]^+$, and C, $\text{Rh}_2(\mu\text{-dpmp})_2(\mu\text{-CO})\text{Br}_2$.

In Figure 6 the geometry within the nearly planar $\text{Rh}_3(\text{CO})_2\text{Cl}_2$ section of 4 is compared with similar structural sections in $[\text{Rh}_3(\mu\text{-dpmp})_2(\text{CO})_3(\mu\text{-Cl})\text{Cl}]^+$,¹ $[\text{Rh}_2(\mu\text{-dpm})_2(\mu\text{-Cl})(\text{CO})_2]^+$,¹² and $\text{Rh}_2(\mu\text{-dpm})_2(\mu\text{-CO})\text{Br}_2$.¹³ The environment of the bridging carbonyl in 4 is similar to that found in $\text{Rh}_2(\mu\text{-dpm})_2(\mu\text{-CO})\text{Br}_2$ and that in $\text{Rh}_2(\mu\text{-Ph}_2\text{Ppy})_2(\mu\text{-CO})\text{Cl}_2$ (Ph_2Ppy is 2-(diphenylphosphino)pyridine).¹⁸ These three bridging carbonyls have rhodium carbon bond lengths which are significantly shorter than other bridging carbonyls. In 4 there is some asymmetry to the Rh_2CO unit with the $\text{Rh}(3)\text{-C}(1)$ distance shorter than the $\text{Rh}(2)\text{-C}(1)$ distance by 0.09 Å. This asymmetry, while greater than that seen in the binuclear counterparts, is not unexpected when the unsymmetrical nature of the entire cation is considered. The $\text{Rh}(3)\text{-Rh}(2)$ distance is shorter than that in $\text{Rh}_2(\mu\text{-dpm})_2(\mu\text{-CO})\text{Br}_2$, longer than the corresponding distance (2.612 (1) Å) in $\text{Rh}_2(\mu\text{-Ph}_2\text{Ppy})_2(\mu\text{-CO})\text{Cl}_2$, and well within the range found for Rh-Rh bonds bridged by carbonyl groups.¹⁸ The bonding to the terminal carbonyl and chloro groups in 4 is unexceptional. The geometry of the bridging chloro group also appears normal. The rhodium chlorine distances have typical values and there is little asymmetry in their lengths. The $\text{Rh}(1)\text{-Cl}(1)\text{-Rh}(2)$ angle is contracted in 4 relative to 2 and $[\text{Rh}_2(\mu\text{-dpm})_2(\mu\text{-Cl})(\text{CO})_2]^+$, and the $\text{Rh}(1)\cdots\text{Rh}(2)$ separation is less in 4 than that in the two other complexes. The Rh-Rh-Rh angle in 4 (136.6 (1)°) is more sharply bent than the corresponding angle (157.4 (1)°) is in 2. Relative to the chloro bridge in 2, Rh(3) has pivoted up by 66°.

Discussion

The trinuclear complex 4 is constructed of structural units familiar from mono- and binuclear complex chemistry. In simple terms, the chemical bonding at rhodium can also be related to that found in these smaller units. The bonding within the $\text{Rh}(2)\text{Rh}(3)\text{P}_4\text{Cl}_2\text{CO}$ unit must be similar to that in $\text{Rh}_2(\mu\text{-dpm})_2(\mu\text{-CO})\text{Br}_2$ and $\text{Rh}_2(\mu\text{-Ph}_2\text{Ppy})_2(\mu\text{-CO})\text{Cl}_2$.¹⁸ Each rhodium in these dinuclear units has a valence count of 16 electrons (eight from Rh(I), two from the terminal halide, four from the trans phosphorus atoms, one from the bridging carbonyl, and one from the Rh-Rh bond). The $\text{Rh}(2)\text{-Rh}(3)$ distance is consistent with cases where direct rhodium-rhodium bonding occurs and is significantly shorter than that found in $\text{Rh}_2(\mu\text{-dpm})_2(\mu\text{-CO})(\mu\text{-EtO}_2\text{CC}_2\text{CO}_2\text{Et})\text{Cl}_2$ (3.3542 Å) where no rhodium-rhodium bond is present.¹⁹ The other rhodium, Rh(1), can be viewed as a loosely appended, 16-electron center which is similar to that found in *trans*- $\text{Rh}(\text{CO})\text{Cl}(\text{PPh}_3)_2$. In electron-counting terms there is no direct bond connecting Rh(1) and Rh(2) and the 2.966 Å separation between these atoms is outside the limits associated with rhodium-rhodium single bonds. However at this distance there must be some rhodium-rhodium interaction, one that is similar to that found in face-to-face rhodium(I) dimers with rhodium-rhodium separations less than 3.5 Å.^{20,21}

As a bridging ligand, dpmp shows considerable flexibility.² It can span a variety of metal-metal separations and accommodate a number of different angular dispositions of those metals and their ligands. In considering the nature of the bridging geometry possible with two equivalent dpmp ligands we have discovered, through the use of space-filling (Corey, Pauling, Koltum) molecular

(18) Farr, J. P.; Olmstead, M. M.; Hunt, C. T.; Balch, A. L. *Inorg. Chem.* 1981, 20, 1182.

(19) Cowie, M.; Southern, T. G. *Inorg. Chem.* 1982, 21, 246.

(20) Balch, A. L. *J. Am. Chem. Soc.* 1976, 98, 8049.

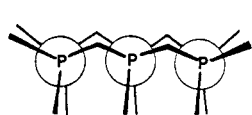
(21) Balch, A. L.; Tulyathan, B. *Inorg. Chem.* 1977, 16, 2840.

Table II. Atom Coordinates (×10⁴) and Temperature Factors (Å² × 10³) for [Rh₃(μ-dpmp)₂(μ-CO)(CO)(μ-Cl)Cl][BPh₄]₂·CH₂Cl₂

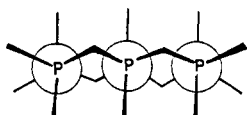
atom	x	y	z	U	atom	x	y	z	U
Rh(1)	1653 (1)	1649 (1)	-412 (1)	17 (1) ^a	C(39)	2215 (7)	755 (10)	1801 (6)	25 (4)
Rh(2)	1250 (1)	3373 (1)	-963 (1)	15 (1) ^a	C(40)	2580 (7)	483 (10)	1465 (6)	28 (4)
Rh(3)	1656 (1)	4460 (1)	-1623 (1)	16 (1) ^a	C(41)	2624 (7)	994 (10)	1037 (5)	21 (4)
Cl(1)	756 (2)	2580 (2)	-394 (1)	20 (1) ^a	C(42)	3128 (7)	2583 (10)	403 (5)	21 (4)
Cl(2)	1709 (2)	5668 (3)	-2171 (2)	26 (1) ^a	C(43)	3504 (7)	2982 (10)	886 (6)	22 (4)
Cl(3)	6355 (3)	7564 (4)	1612 (3)	104 (3) ^a	C(44)	4154 (7)	3160 (10)	940 (6)	31 (4)
Cl(4)	5580 (3)	8983 (4)	1065 (3)	99 (3) ^a	C(45)	4405 (7)	2966 (11)	505 (6)	32 (4)
P(1)	987 (2)	863 (3)	-1122 (2)	17 (1) ^a	C(46)	4044 (7)	2588 (11)	24 (6)	30 (4)
P(2)	564 (2)	2665 (3)	-1683 (2)	17 (1) ^a	C(47)	3386 (7)	2394 (10)	-17 (6)	26 (4)
P(3)	1092 (2)	3730 (3)	-2400 (2)	17 (1) ^a	C(48)	2569 (6)	4633 (9)	-277 (5)	15 (3)
P(4)	2287 (2)	2404 (3)	331 (2)	18 (1) ^a	C(49)	1388 (6)	5109 (9)	-58 (5)	14 (3)
P(5)	1818 (2)	4178 (3)	-227 (2)	17 (1) ^a	C(50)	1707 (7)	5718 (10)	312 (6)	24 (4)
P(6)	2381 (2)	5215 (3)	-932 (2)	18 (1) ^a	C(51)	1380 (7)	6451 (10)	451 (6)	29 (4)
O(1)	2388 (4)	2864 (6)	-1232 (4)	21 (2)	C(52)	713 (7)	6535 (10)	193 (6)	27 (4)
O(2)	2634 (5)	266 (7)	-302 (4)	42 (3)	C(53)	407 (8)	5931 (11)	-180 (7)	42 (5)
C(1)	1965 (6)	3354 (10)	-1276 (5)	19 (3)	C(54)	753 (7)	5203 (10)	-316 (6)	32 (4)
C(2)	2252 (7)	813 (10)	-361 (6)	22 (4)	C(55)	3161 (6)	5309 (9)	-1045 (5)	15 (3)
C(3)	326 (6)	1536 (9)	-1553 (5)	17 (3)	C(56)	3557 (7)	4548 (10)	-956 (5)	24 (4)
C(4)	552 (7)	-11 (10)	-911 (5)	20 (4)	C(57)	4159 (7)	4632 (11)	-1053 (6)	34 (4)
C(5)	22 (7)	-406 (10)	-1260 (5)	24 (4)	C(58)	4341 (7)	5418 (11)	-1249 (6)	35 (4)
C(6)	-309 (7)	-1105 (11)	-1078 (6)	36 (4)	C(59)	3933 (7)	6141 (10)	-1349 (6)	30 (4)
C(7)	-109 (8)	-1357 (11)	-544 (6)	37 (5)	C(60)	3335 (7)	6094 (10)	-1240 (6)	23 (4)
C(8)	407 (7)	-956 (10)	-203 (6)	30 (4)	C(61)	2180 (7)	6341 (9)	-783 (5)	20 (4)
C(9)	755 (7)	-288 (10)	-367 (6)	25 (4)	C(62)	2656 (7)	6875 (9)	-420 (5)	20 (4)
C(10)	1350 (6)	428 (9)	-1610 (5)	18 (4)	C(63)	2486 (7)	7733 (9)	-290 (5)	20 (4)
C(11)	1900 (6)	839 (9)	-1660 (5)	19 (4)	C(64)	1862 (7)	8059 (10)	-515 (6)	23 (4)
C(12)	2147 (7)	603 (10)	-2083 (6)	27 (4)	C(65)	1400 (7)	7501 (10)	-864 (6)	27 (4)
C(13)	1835 (7)	-46 (11)	-2454 (6)	34 (4)	C(66)	1563 (7)	6640 (10)	-1002 (5)	22 (4)
C(14)	1277 (7)	-462 (11)	-2406 (6)	36 (4)	C(67)	3787 (7)	6542 (10)	1209 (5)	24 (4)
C(15)	1025 (7)	-249 (10)	-1985 (6)	32 (4)	C(68)	4103 (7)	7235 (11)	1020 (6)	33 (4)
C(16)	831 (6)	2591 (9)	-2280 (5)	15 (3)	C(69)	4384 (7)	7126 (11)	595 (6)	37 (5)
C(17)	-193 (6)	3201 (9)	-1905 (5)	18 (4)	C(70)	4335 (7)	6279 (11)	335 (6)	37 (5)
C(18)	-348 (7)	3795 (10)	-1554 (6)	24 (4)	C(71)	4039 (7)	5594 (10)	525 (6)	28 (4)
C(19)	-936 (7)	4256 (10)	-1708 (6)	32 (4)	C(72)	3757 (7)	5722 (10)	953 (6)	23 (4)
C(20)	-1370 (7)	4098 (10)	-2205 (6)	29 (4)	C(73)	3290 (7)	5750 (10)	1899 (6)	24 (4)
C(21)	-1205 (7)	3480 (10)	-2555 (6)	25 (4)	C(74)	2687 (7)	5359 (10)	1681 (6)	24 (4)
C(22)	-620 (7)	3017 (9)	-2411 (5)	21 (4)	C(75)	2553 (6)	4483 (10)	1807 (5)	19 (4)
C(23)	376 (7)	4222 (10)	-2833 (6)	23 (4)	C(76)	3033 (7)	3955 (10)	2160 (6)	30 (4)
C(24)	68 (7)	3786 (10)	-3338 (6)	24 (4)	C(77)	3637 (7)	4331 (10)	2390 (6)	27 (4)
C(25)	-488 (7)	4177 (10)	-3683 (6)	28 (4)	C(78)	3763 (7)	5227 (10)	2260 (6)	29 (4)
C(26)	-740 (7)	4963 (10)	-3528 (6)	28 (4)	C(79)	2824 (7)	7365 (10)	1502 (6)	27 (4)
C(27)	-419 (7)	5361 (10)	-3014 (6)	29 (4)	C(80)	2356 (7)	7353 (10)	1774 (6)	28 (4)
C(28)	130 (6)	5001 (9)	-2686 (5)	17 (4)	C(81)	1811 (7)	7918 (10)	1618 (6)	31 (4)
C(29)	1618 (6)	3540 (9)	-2816 (5)	19 (4)	C(82)	1729 (7)	8514 (10)	1178 (6)	31 (4)
C(30)	2121 (7)	2949 (10)	-2623 (6)	22 (4)	C(83)	2186 (7)	8546 (11)	906 (6)	37 (5)
C(31)	2564 (7)	2826 (10)	-2927 (6)	28 (4)	C(84)	2716 (7)	7951 (10)	1046 (6)	32 (4)
C(32)	2488 (7)	3314 (11)	-3403 (6)	34 (4)	C(85)	3987 (7)	7269 (10)	2216 (6)	24 (4)
C(33)	1976 (7)	3893 (11)	-3593 (6)	34 (4)	C(86)	4638 (7)	7079 (10)	2339 (6)	29 (4)
C(34)	1543 (7)	4027 (11)	-3297 (6)	32 (4)	C(87)	5081 (7)	7499 (11)	2789 (6)	32 (4)
C(35)	2005 (6)	3540 (9)	410 (5)	16 (3)	C(88)	4884 (7)	8095 (11)	3112 (6)	35 (4)
C(36)	2293 (6)	1824 (9)	939 (5)	16 (3)	C(89)	4230 (7)	8289 (11)	2983 (6)	35 (4)
C(37)	1943 (7)	2127 (10)	1287 (6)	22 (4)	C(90)	3787 (7)	7878 (10)	2533 (6)	26 (4)
C(38)	1924 (7)	1587 (10)	1725 (6)	28 (4)	C(91)	5747 (9)	8259 (14)	1641 (8)	63 (6)
					B	3460 (8)	6734 (12)	1705 (7)	28 (5)

^a Equivalent isotropic *U* defined as one-third of the trace of the orthogonalized *U*_{*ij*} tensor.

models, that two arrangements of these ligands in a trans, fully aligned fashion are possible. These are shown in Newman projections down the P-Rh-P axes as 5 and 6.



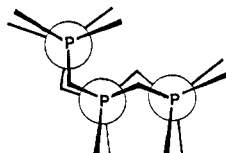
5



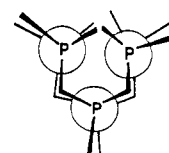
6

In 5 with its fully extended PCPCP chain, the Rh₃(μ-dpmp)₂ unit has idealized C_{2v} symmetry which places a mirror plane that contains the three rhodium atoms perpendicular to the PRhP units. In 6 however the symmetry of this unit is only C_i with the central rhodium atom lying at the center of symmetry. Arrangement 6 is relatively inflexible and has not been found in any of the dpmp-

bridged structures examined to date. In contrast, 5 is highly flexible. In particular, simultaneous rotation of two opposing methylene groups allows for conformation change into the kinked structure 7. A second such rotation



7



8

performed on 7 leads to the bent structure 8 without requiring rupture of either rhodium-phosphorus or carbon-phosphorus bonds. The motion of the phosphine ligands in this process is similar to that involved in A-frame inversion of dpm-bridged structures.²²⁻²⁴ The extended

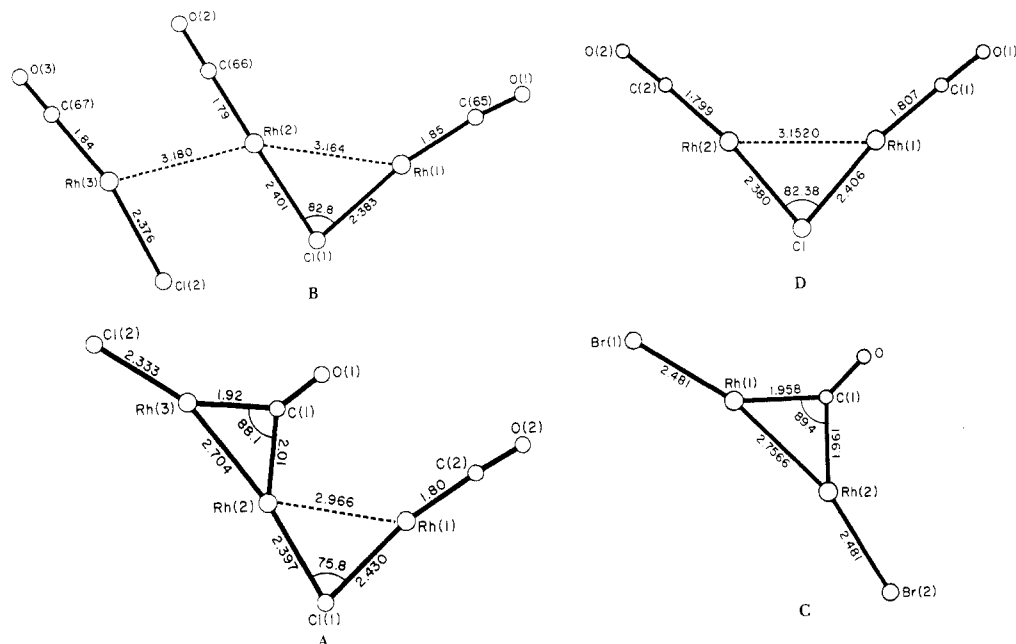


Figure 6. A comparison of corresponding planar sections of A, $[\text{Rh}_3(\mu\text{-dpmp})_2(\mu\text{-CO})(\text{CO})(\mu\text{-Cl})\text{Cl}]^+$, B, $[\text{Rh}_3(\mu\text{-dpmp})_2(\text{CO})_3(\mu\text{-Cl})\text{Cl}]^+$, C, $\text{Rh}_2(\mu\text{-dpm})_2(\mu\text{-CO})\text{Br}_2$, and D, $[\text{Rh}_2(\mu\text{-dpm})_2(\mu\text{-Cl})(\text{CO})_2]^+$.

Table III. Selected Interatomic Distances (Å) for $[\text{Rh}_3(\mu\text{-dpmp})_2(\mu\text{-CO})(\text{CO})(\mu\text{-Cl})\text{Cl}][\text{BPh}_4] \cdot \text{CH}_2\text{Cl}_2$

At Rh(1)			
Rh(1)-Cl(1)	2.430 (4)	Rh(1)-P(1)	2.322 (4)
Rh(1)-P(4)	2.324 (4)	Rh(1)-C(2)	1.797 (15)
Rh(1)-Rh(2)	2.966 (1)		
At Rh(2)			
Rh(2)-Rh(3)	2.704 (2)	Rh(2)-Cl(1)	2.397 (4)
Rh(2)-P(2)	2.299 (4)	Rh(2)-P(5)	2.304 (4)
Rh(2)-C(1)	1.973 (15)		
At Rh(3)			
Rh(3)-Rh(2)	2.704 (2)	Rh(3)-Cl(2)	2.333 (4)
Rh(3)-P(3)	2.320 (4)	Rh(3)-P(6)	2.323 (4)
Rh(3)-C(1)	1.917 (14)		
At Carbon Monoxide			
O(2)-C(2)	1.153 (18)	O(1)-C(1)	1.166 (17)
At Phosphorus			
P(1)-C(4)	1.802 (16)	P(1)-C(3)	1.855 (13)
P(2)-C(3)	1.833 (15)	P(1)-C(10)	1.812 (16)
P(2)-C(17)	1.788 (14)	P(2)-C(16)	1.821 (16)
P(3)-C(23)	1.807 (13)	P(3)-C(16)	1.859 (14)
P(4)-C(35)	1.847 (14)	P(3)-C(29)	1.825 (16)
P(4)-C(42)	1.826 (15)	P(4)-C(36)	1.806 (14)
P(5)-C(48)	1.829 (15)	P(5)-C(35)	1.856 (14)
P(6)-C(48)	1.856 (14)	P(5)-C(49)	1.812 (15)
P(6)-C(61)	1.817 (15)	P(6)-C(55)	1.832 (15)

conformation **5** allows for a nearly linear array of the three metal ions, and it is significant that the two dpmp-bridged structures with largest Rh-Rh-Rh angles, **2** ($156.1(4)^\circ$) and $[\text{Rh}_3(\mu\text{-dpmp})_2(\mu\text{-CO})_2(\text{CO})(\mu\text{-S}_2\text{COEt})(\text{S}_2\text{COEt})_2]$ ($170.5(1)^\circ$),³ have the phosphine ligands arranged in this fashion. In contrast the kinked structure **6** requires bending of the Rh_3 unit. $[\text{Rh}_3(\mu\text{-dpmp})_2(\mu\text{-CO})(\text{CO})(\mu\text{-Cl})\text{Cl}]^+$, **4**, has this kinked structure. Because it is possible to convert **5** into **7** simply by rotation about two trans methylene groups, it is possible for the decarbonylation

reaction, which converts **2** into **4**, to proceed without the need for dissociation of any part of the phosphine ligand from the $\text{Rh}_3(\mu\text{-dpmp})_2$ core.²⁵ However, that does not ensure that the rhodium phosphorus bonds remain intact throughout the decarbonylation reaction. We have recently reported on several reactions of polynuclear phosphine-bridged complexes in which metal-phosphorus bonds must be broken.²⁵⁻²⁷

All of the available data indicate that the three halo complexes $[\text{Rh}_3(\mu\text{-dpmp})_2(\mu\text{-CO})(\text{CO})(\mu\text{-X})\text{X}]^+$ have the same structure. These may be considered as coordinatively unsaturated species, and it appears that they are reasonably reactive toward the addition of small molecules. Carbon monoxide reacts to form the corresponding tricarbonyls. It is interesting to note that, although all of the dicarbonyls possess similar structure, the addition of carbon monoxide converts them into tricarbonyls with the three unique structures which were described in the Introduction. Other small molecules, including sulfur dioxide, acetylenes bearing electronegative substituents, and isocyanides, add to these dicarbonyls. Studies of the chemical reactivity and structures of these adducts are in progress.

Experimental Section

Preparation of Compounds. Dpmp^{28} and the complexes $[\text{Rh}_2(\mu\text{-dpmp})_2(\text{CO})_3\text{X}_2]\text{BPh}_4$ ($\text{X} = \text{Cl}, \text{Br}, \text{I}^2$) were prepared as described previously.

$[\text{Rh}_3(\mu\text{-dpmp})_2(\mu\text{-CO})(\text{CO})(\mu\text{-Cl})\text{Cl}][\text{BPh}_4] \cdot \text{CH}_2\text{Cl}_2$. A violet solution of 340 mg of $[\text{Rh}_3(\mu\text{-dpmp})_2(\text{CO})_3\text{Cl}_2][\text{BPh}_4]$ in 60 mL of acetonitrile was heated under reflux for 48 h under an inert atmosphere. The red-brown solution then was evaporated to dryness, and the resulting red-brown, oily residue was dissolved in ca. 15 mL of acetone and allowed to stand for 1 h. The solution was filtered to remove a rose solid (starting material). Addition of diethyl ether to the filtrate produced red crystals of the product which was collected by filtration and washed with ether. Puri-

(22) Balch, A. L.; Hunt, C. T.; Lee, C. L.; Olmstead, M. M.; Farr, J. P. *J. Am. Chem. Soc.* **1981**, *103*, 3764.

(23) Lee, C. L.; Hunt, C. T.; Balch, A. L. *Organometallics* **1982**, *1*, 824.

(24) Puddephatt, R. J.; Azam, K. A.; Hill, R. M.; Brown, M. P.; Nelson, C. D.; Mouldings, R. P.; Seddon, K. R.; Grossel, M. C. *J. Am. Chem. Soc.* **1983**, *105*, 5642.

(25) Wood, F. E.; Hvoslef, J.; Balch, A. L. *J. Am. Chem. Soc.* **1983**, *105*, 6986.

(26) Farr, J. P.; Wood, F. E.; Balch, A. L. *Inorg. Chem.* **1983**, *22*, 3387.

(27) Farr, J. P.; Olmstead, M. M.; Rutherford, N. M.; Wood, F. E.; Balch, A. L. *Organometallics* **1983**, *2*, 1758.

(28) Appel, R.; Geisler, K.; Scholer, M.-F. *Chem. Ber.* **1979**, *112*, 648.

Table IV. Selected Interatomic Angles (deg) for [Rh₃(μ-dpmp)₂(μ-CO)(CO)(μ-Cl)Cl][BPh₄] \cdot CH₂Cl₂

		At Rh(1)			
Cl(1)-Rh(1)-P(1)	88.8 (1)	P(1)-Rh(1)-C(2)	89.0 (4)	Cl(1)-Rh(1)-C(2)	169.4 (5)
P(1)-Rh(1)-P(4)	176.7 (2)	Cl(1)-Rh(1)-P(4)	89.9 (1)	P(4)-Rh(1)-C(2)	91.7 (4)
		At Rh(2)			
Rh(3)-Rh(2)-Cl(1)	170.8 (1)	P(2)-Rh(2)-C(1)	94.0 (4)	P(2)-Rh(2)-P(5)	172.2 (2)
Cl(1)-Rh(2)-P(2)	88.1 (1)	Rh(1)···Rh(2)-Rh(3)	136.6 (1)	Cl(1)-Rh(2)-C(1)	144.1 (4)
Cl(1)-Rh(2)-P(5)	88.7 (1)	Rh(3)-Rh(2)-P(2)	91.1 (1)	P(95)-Rh(2)-C(1)	92.8 (4)
Rh(3)-Rh(2)-C(1)	45.1 (4)	Rh(3)-Rh(2)-P(5)	90.9 (1)		
		At Rh(3)			
Rh(2)-Rh(3)-Cl(2)	160.7 (1)	P(3)-Rh(3)-C(1)	91.7 (4)	P(3)-Rh(3)-P(6)	168.3 (2)
Cl(2)-Rh(3)-P(3)	86.6 (1)	Rh(2)-Rh(3)-P(3)	94.5 (1)	Cl(2)-Rh(3)-C(1)	152.5 (5)
Cl(2)-Rh(3)-P(6)	87.2 (1)	Rh(2)-Rh(3)-P(6)	94.6 (1)	P(6)-Rh(3)-C(1)	89.3 (4)
Rh(2)-Rh(3)-C(1)	46.8 (5)				
		Bridge Atoms			
Rh(1)-Cl(1)-Rh(2)	75.8 (1)	Rh(2)-C(1)-Rh(3)	88.1 (6)		
		Methylene Carbons			
P(1)-C(3)-P(2)	113.5 (7)	P(2)-C(16)-P(3)	106.3 (7)	P(5)-C(48)-P(6)	106.1 (6)
P(4)-C(35)-P(5)	111.7 (7)				
		Carbonyl Groups			
Rh(1)-C(2)-O(2)	176.3 (4)	Rh(2)-C(1)-O(1)	132.8 (12)	Rh(3)-C(1)-O(1)	139.1 (12)
		At Phosphorus			
Rh(1)-P(1)-C(3)	114.1 (4)	Rh(2)-P(5)-C(35)	113.6 (4)	Rh(3)-P(3)-C(23)	120.1 (5)
C(3)-P(1)-C(4)	100.9 (6)	C(35)-P(5)-C(48)	106.7 (6)	Rh(3)-P(3)-C(29)	108.8 (4)
C(3)-P(1)-C(10)	101.5 (6)	C(35)-P(5)-C(49)	100.1 (6)	C(23)-P(3)-C(29)	106.3 (7)
Rh(2)-P(2)-C(3)	115.6 (4)	Rh(3)-P(6)-C(48)	113.8 (4)	Rh(1)-P(4)-C(36)	110.3 (4)
C(3)-P(2)-C(16)	106.4 (7)	C(48)-P(6)-C(55)	102.4 (6)	Rh(1)-P(4)-C(42)	120.2 (5)
C(3)-P(2)-C(17)	100.7 (6)	C(48)-P(6)-C(61)	104.1 (6)	C(36)-P(4)-C(42)	103.4 (6)
Rh(3)-P(3)-C(16)	113.6 (4)	Rh(1)-P(1)-C(4)	113.2 (5)	Rh(2)-P(5)-C(48)	114.7 (5)
C(16)-P(3)-C(23)	103.0 (6)	Rh(1)-P(1)-C(10)	116.0 (4)	Rh(2)-P(5)-C(49)	114.3 (4)
C(16)-P(3)-C(29)	103.7 (7)	C(4)-P(1)-C(10)	109.6 (7)	C(48)-P(5)-C(49)	106.1 (6)
Rh(1)-P(4)-C(35)	113.8 (4)	Rh(2)-P(2)-C(16)	115.3 (4)	Rh(3)-P(6)-C(55)	112.1 (4)
C(35)-P(4)-C(36)	105.2 (7)	Rh(2)-P(2)-C(17)	112.7 (5)	Rh(3)-P(6)-C(61)	117.7 (4)
C(35)-P(4)-C(42)	102.5 (6)	C(16)-P(2)-C(17)	104.7 (6)	C(55)-P(6)-C(61)	105.1 (7)

fication was achieved by recrystallization from dichloromethane/diethyl ether: yield 210 mg (62%). Anal. Calcd for C₉₁H₈₀BCl₄O₂P₆Rh₃: C, 58.99; H, 4.35; Cl, 7.65; P, 10.03. Found: C, 58.29; H, 4.76; Cl, 8.36; P, 9.92.

[Rh₃(μ-dpmp)₂(μ-CO)(CO)(μ-Br)(Br)][BPh₄]. A solution containing 265 mg of [Rh₃(μ-dpmp)₂(CO)₃Br₂][BPh₄] in 40 mL of acetone was heated under reflux for 12 h under an inert atmosphere. The red-brown solution was evaporated to dryness using a rotary evaporator. The solid residue was dissolved in a minimum volume of acetone and filtered. Diethyl ether was slowly added to the filtrate until most of the product had precipitated as large red-black crystals. The mixture was stored at -10 °C for 2 h, and then the product was recovered by filtration. It was further purified by recrystallization from dichloromethane/ether: yield 199 mg (76%). Anal. Calcd for C₉₀H₇₈BBR₂O₂P₆Rh₃: C, 58.22; H, 4.23; Br, 8.61. Found: C, 58.20; H, 3.73; Br, 8.84. A sample of [Rh₃(μ-dpmp)₂(μ-CO)(CO)(μ-Br)Br][BPh₄] which was ca. 70% enriched in ¹³C was prepared by an exchange reaction between 98% enriched ¹³CO and [Rh₃(μ-dpmp)₂(CO)₃Cl₂][BPh₄] in dichloromethane solution over a 12-h period, followed by metathesis with NaBr to give [Rh₃(μ-dpmp)₂(¹³CO)₃Br₂][BPh₄] which was then subjected to thermal decarbonylation.

[Rh₃(μ-dpmp)₂(CO)(μ-I)(I)][BPh₄]. A brown solution of 210 mg of [Rh₃(μ-dpmp)₂(μ-CO)(CO)₂(μ-I)₂][BPh₄] in 60 mL of acetone was heated under reflux for 48 h. The red brown solution was evaporated to dryness, and the solid residue was recrystallized twice by dissolving it in a minimum volume of dichloromethane, filtering, and then slowly adding ether: yield 150 mg (72%). Anal. Calcd for C₉₀H₇₈BI₂O₂P₆Rh₃: C, 55.41; H, 4.03; I, 13.01; P, 9.53. Found: C, 55.14; H, 4.25; I, 12.34; P, 9.01.

Spectroscopic Measurements. The ³¹P and ¹H NMR spectra were recorded at 145.8 and 360 MHz, respectively, on a Nicolet NT-360 Fourier transform spectrometer. The ³¹P and ¹³C NMR spectra were recorded at 81 and 50.3 MHz, respectively, on a Nicolet 200 Fourier transform spectrometer. All ³¹P NMR spectra were proton decoupled, and an external 85% phosphoric acid reference was used. Tetramethylsilane was the reference for both ¹H and ¹³C NMR spectra. The high-frequency-positive convention,

Table V. Crystal Data for [Rh₃(μ-dpmp)₂(μ-CO)(CO)(μ-Cl)(Cl)][BPh₄] \cdot CH₂Cl₂

formula	C ₉₁ H ₈₀ BCl ₄ O ₂ P ₆ Rh ₃
fw dimer + solvent	1772.26
cryst system	monoclinic
space group	P2 ₁ /n
based on conditns	0k0, k = 2n; h0l, h + l = 2n
cryst dimens, mm	0.370 × 0.325 × 0.070
color and habit	red plates
unit cell dimens (140 K)	
a, Å	22.015 (8)
b, Å	15.002 (4)
c, Å	106.95 (2)
V, Å ³	8240 (4)
d, g cm ⁻³ (20 °C)	1.52
d(calcd), g cm ⁻³ (140 K)	1.43
Z	4
radiatn λ, Å (graphite monochromator)	Mo Kα
μ(Mo Kα), cm ⁻¹	Mo, 0.710 69
range of abs correctn factors	8.66
scan type 2θ max, deg	1.05-1.27
scan range, deg	ω, 45
background offset, deg	1.0
octants	±1.0
scan speed, deg min ⁻¹	h, k, ±l
check reflectn, interval no.	15
no. of unique data	2 measured every 200 reflectns
no. of data I > 2σ(I)	10 767
R	7796
R _w	0.072
no. of parameters	0.067
	495

recommended by IUPAC, has been used in reporting all chemical shifts. Infrared spectra were recorded from dichloromethane solutions using a Perkin-Elmer 180 spectrometer. Electronic spectra were obtained by using a Hewlett-Packard 8450A spectrometer.

The ^{31}P NMR spectrum shown in Figure 2 was simulated by using the 1180/1280 ITRCAL routine (an adaptation of the Laocoon III) of the Nicolet software. This routine is designed for simulation of systems with a maximum of seven nuclei with spin $1/2$. Since our complexes involve six phosphorus and three rhodium atoms (nine spin $1/2$ nuclei in all), we had to carry out the calculations in three parts. To do this we performed individual simulations using all six phosphorus atoms, with full coupling between them, and one rhodium atom which was placed at Rh_a , Rh_b , and Rh_c in successive calculations.²⁹ As a result the calculations cannot include any Rh-Rh coupling nor can they include Rh-P coupling other than one-bond coupling. However this is not a major limitation since these particular coupling constants are known from work on simpler molecules to be much smaller (<10 Hz) than most of the coupling constants used in the simulations.¹⁸ The calculations produced satisfactory simulations of the spectra at both 145.8 and 81 MHz.

X-ray Data Collection, Refinement, and Solution. Well-formed red crystals were obtained by slow vapor diffusion of diethyl ether into a dichloromethane solution of $[\text{Rh}_3(\mu\text{-dpmp})_2(\mu\text{-CO})(\text{CO})(\mu\text{-Cl})(\text{Cl})][\text{BPh}_4]$. Crystal data, data collection procedure, and refinement of the structure are summarized in Table V. The lattice was found to be monoclinic by standard procedures using the software associated with the Syntex P₂ diffractometer. Quick scans of the reflections for space group determination yielded the conditions $0k0$, $k = 2n$, and $h0l$, $h + l = 2n$, consistent with the space group $P2_1/n$. The data were collected at 140 K by using a locally modified LT-1 low-temperature apparatus on the Syntex P₂ diffractometer. The data were corrected for Lorentz, polarization, and extinction effects.

The structure was solved by locating the three rhodium atoms using the Patterson map generated using the FMAP8 routine of SHELXTL, version 4, 1984 (Nicolet Instrument Corporation, Madison, WI). Other atoms were located from successive difference Fourier maps. Final cycles of refinement were made with anisotropic thermal parameters for rhodium, phosphorus, and chlorine and isotropic thermal parameters for all remaining atoms. Hydrogen atoms were not located. Scattering factors and corrections for anomalous dispersion was taken from a standard source.³⁰ An absorption correction (XABS) was applied. A conventional R factor of 0.072 was obtained. The final difference Fourier map showed a feature at 0.532, 0.071, 0.025 ($3.4 \text{ e } \text{\AA}^{-3}$) which was 1.33 \AA away from a feature at 0.5, 0, 0 ($2.3 \text{ e } \text{\AA}^{-3}$). These produce a linear triatomic molecule (by inversion of the first peak) which may represent a disordered remnant of a solvent molecule which largely vaporized from the crystal.

Acknowledgment. We thank the National Science Foundation (No. CHE8217954) for financial support and Mr. M. V. Nguyen for experimental assistance.

Registry No. 2, 84774-75-4; 3, 86372-62-5; 4 (X = Cl), 95045-36-6; 4 (X = Br), 95045-39-9; 4 (X = I), 95045-41-3; 4- CH_2Cl (X = Cl), 95045-37-7; $[\text{Rh}_3(\mu\text{-dpmp})_2(^{13}\text{C})_3\text{Br}_2][\text{BPh}_4]$, 95045-43-5; $[\text{Rh}_3(\mu\text{-dpmp})_2(\text{CO})_3\text{Br}_2][\text{BPh}_4]$, 95045-45-7.

Supplementary Material Available: A listing of anisotropic thermal parameters, hydrogen atom positions, and structure factor amplitudes (31 pages). Ordering information is given on any current masthead page.

(29) Guimerans, R. R. Ph.D. Thesis, University of California, Davis, 1983.

(30) "International Tables for X-ray Crystallography"; Kynoch Press: Birmingham, England, 1974; Vol. IV, pp 99, 149.

Transition-Metal Ketenes. 25.¹

Bis(trimethylphosphine)-Substituted η^2 -Alkyne Complexes of Tungsten. Synthesis, Structure, and Extended Hückel MO Calculations

Fritz R. Kreissl,* Werner J. Sieber, Peter Hofmann,* Jürgen Riede, and Mathias Wolfgruber

Anorganisch-chemisches Institut der Technischen Universität München, D-8046 Garching, West Germany

Received August 13, 1984

Bis(trimethylphosphine)-substituted, cationic η^2 -alkyne complexes of tungsten ($\eta^5\text{-C}_5\text{H}_5$) $[\text{P}(\text{CH}_3)_3]_2\text{W}(\eta^2\text{-RC}\equiv\text{COR}')[\text{BF}_4]$ (R = CH_3 , $\text{C}_6\text{H}_4\text{CH}_3$ -4; R' = CH_3 , C_6H_5) were prepared by treatment of the corresponding mixed carbonyl-trimethylphosphine alkyne complexes with trimethylphosphine. The substitution is accompanied by an unexpected color change from yellow to violet which can be explained on the basis of extended Hückel MO calculations. The structures of the new compounds were determined by spectroscopy and, in the case of the η^2 -methoxy(4-methylphenyl)ethyne complex **2b**, additionally by X-ray analysis.

Introduction

The intramolecular carbonylation of suitable carbyne complexes leads via CC bond formation to η^1 - and η^2 -ketenyl complexes.²⁻⁵ These show pronounced reactivity toward Lewis basis to afford new ketenyl,^{4,5} σ -bonded

alkynyl,⁶ arsino- and phosphinoketene^{7,8} as well as η^3 -phosphinoketene complexes.^{9,10} On the other hand, the η^2 -ketenyl complexes add Lewis acids to the ketene oxygen atom with concomitant conversion of the η^2 -ketenyl into an η^2 -alkyne ligand. This reaction allows an easy access

(1) Contribution 24: Kreissl, F. R.; Wolfgruber, M.; Sieber, W. J. *J. Organomet. Chem.* 1984, 270, C4.

(2) Kreissl, F. R.; Frank, A.; Schubert, U.; Lindner, T. L.; Huttner, G. *Angew. Chem.* 1976, 88, 649; *Angew. Chem., Int. Ed. Engl.* 1976, 15, 632.

(3) Kreissl, F. R.; Friedrich, P.; Huttner, G. *Angew. Chem.* 1977, 89, 110; *Angew. Chem., Int. Ed. Engl.* 1977, 16, 102.

(4) Kreissl, F. R.; Uedelhoven, W.; Eberl, K. *Angew. Chem.* 1978, 90, 908; *Angew. Chem., Int. Ed. Engl.* 1978, 17, 859.

(5) Uedelhoven, W.; Eberl, K.; Kreissl, F. R. *Chem. Ber.* 1979, 112, 3376.

(6) Kreissl, F. R.; Eberl, K.; Uedelhoven, W. *Angew. Chem.* 1978, 90, 908; *Angew. Chem., Int. Ed. Engl.* 1978, 17, 860.

(7) Kreissl, F. R.; Wolfgruber, M.; Sieber, W.; Alt, H. G. *Angew. Chem.* 1983, 95, 159; *Angew. Chem., Int. Ed. Engl.* 1983, 22, 149; *Angew. Chem. Suppl.* 1983, 148.

(8) Wolfgruber, M.; Sieber, W.; Kreissl, F. R. *Chem. Ber.* 1984, 117, 427.

(9) Kreissl, F. R.; Wolfgruber, M.; Sieber, W.; Ackermann, K. *J. Organomet. Chem.* 1983, 252, C39.

(10) Kreissl, F. R.; Wolfgruber, M.; Sieber, W.; Ackermann, K. *Organometallics* 1984, 3, 777.